An Unstructured Finite Element Solver for Ship Hydrodynamics Problems

J. García, E. Oñate

A stabilized semi-implicit fractional step algorithm based on the finite element method for solving ship wave problems using unstructured meshes is presented. The stabilized gov-erning equations for the viscous incompressible fluid and the free surface are derived at a differential level via a finite calculus procedure. This allows us to obtain a stabilized numerical solution scheme. Some particular aspects of the problem solution, such as the mesh updating procedure and the transom stern treatment, are presented. Examples of the efficiency of the semi-implicit algorithm for the analysis of ship hydrodynamics problems are presented.

Introduction

The prediction of the wave pattern and resistance joint to the study of the flow around a ship are topics of major relevance in naval architecture. The analytical and numerical solutions of this problem have challenged mathematicians and hydrodynamicists for over a century.

Despite recent advances in computational fluid dynamics (CFD) methods and computer hardware, the numerical solutions of ship wave problems is still a challenge. This is mainly due to the difficulties in solving the incompressible flow equations coupled to the free boundary constraint stating that at this boundary the fluid particles must remain on the water surface, whose position is in turn unknown.

This paper presents advances in recent work of the authors, [1–10], to derive a stabilized finite element method which allows us to overcome the above mentioned problems. The starting points are the modified governing differential equations for the incompressible flow and the free surface condition incorporating the necessary stabilization terms via a *finite calculus* (FIC) procedure developed by the authors, [8–10]. The FIC technique is based on writing the different balance equations over a domain of finite size and retaining higher order terms. These terms incorporate the ingredients for the necessary stabilization of any transient and steady-state numerical solution *already at the differential equations level*. In addition, the modified differential equations can be used to derive a numerical scheme for computing the stabilization parameters, [5,6,7,9].

The stabilized differential equations are first solved in time using a semi-implicit fractional step approach. Application of the standard Galerkin finite element formulation to the fractional steps equations leads to a stabilized system of discretized equations which overcomes the above-mentioned problems, allowing for equal order linear interpolations of the velocity and pressure variables over the elements. Unstructured grids of linear tetrahedra have been used in this work. The approach is similar to semi-implicit fractional methods proposed in [11–13]. The particular features of the algorithm here proposed are the additional stabilization terms introduced by the FIC formulation. These terms ensure the stabilization of the algorithm for small time-step sizes and enhance the convergence towards the steady-state solution. Free surface wave boundary effects are accounted for in the flow solution either by moving the free surface nodes in a Lagrangean manner, or else for via the introduction of a prescribed pressure at the free surface computed from the wave height.

The content of the paper is structured as follows. First the stabilized semi-implicit fractional step approach using the finite element method is then described. Details of the computation of the stabilization parameters are also given. Finally some examples of applications of the unstructured-grid solver for ship hydrodynamics problems are presented.

Finite Calculus (FIC) Formulation of Viscous Turbulent Flow and Free Surface Equations

We consider the motion around a body of a viscous incompressible fluid including a free surface.

The finite calculus form of the governing differential equations for the three-dimensional problem can be written as, [8–10] follows:

Momentum

$$r_{m_i} - \frac{1}{2} h_j \frac{\partial r_{m_i}}{\partial x_j} = 0 \quad \text{on} \quad \Omega \quad i,j = 1,2,3 \tag{1}$$

Mass Balance

$$r_d - \frac{1}{2} h_j \frac{\partial r_d}{\partial x_j} = 0 \quad \text{on} \quad \Omega \quad j = 1,2,3 \tag{2}$$

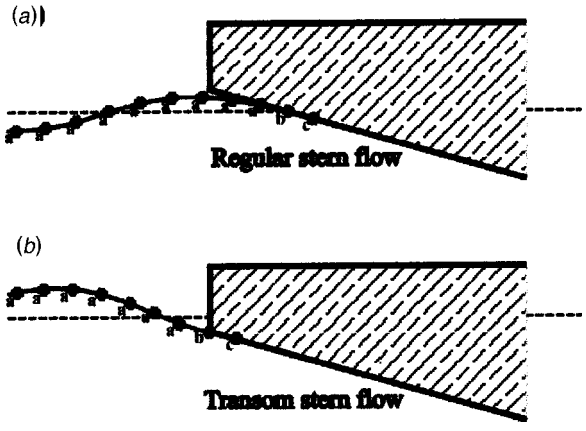

Fig. 1 Transom stern model. (*a*) Regular stern flow, (*b*) transom stern flow.

Contributed by the Applied Mechanics Division of THE AMERICAN SOCIETY OF MECHANICAL ENGINEERS for publication in the ASME JOURNAL OF APPLIED MECHANICS. Manuscript received by the Applied Mechanics Division, July 26, 2001; final revision, Mar. 12, 2002. Associate Editor: T. E. Tezduyar. Discussion on the paper should be addressed to the Editor, Prof. Robert M. McMeeking, Chair, Department of Mechanics and Environmental Engineering, University of California—Santa Barbara, Santa Barbara, CA 93106-5070, and will be accepted until four months after final publication in the paper itself in the ASME JOURNAL OF APPLIED MECHANICS.

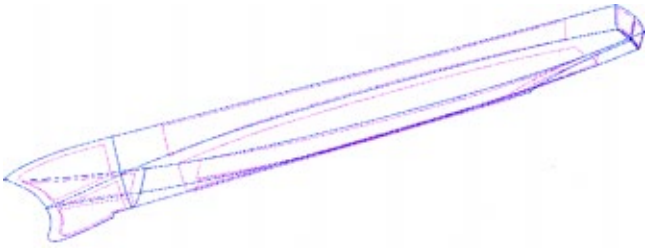

Fig. 2 DTMB 5415 model. Geometrical definition based on NURBS surfaces.

Fig. 3 DTMB 5415 model. Surface mesh used in the analysis.

Free Surface

$$r_\beta - \frac{1}{2} h_{\beta_j} \frac{\partial r_\beta}{\partial x_j} = 0 \quad \text{on} \quad \Gamma_\beta \quad j = 1,2 \tag{3}$$

where

$$r_{m_i} = \frac{\partial u_i}{\partial t} + \frac{\partial}{\partial x_j}(u_i u_j) + \frac{\partial p}{\partial x_i} - \frac{\partial \tau_{ij}}{\partial x_j}$$

$$r_d = \frac{\partial u_i}{\partial x_i}, \quad i = 1,2,3$$

$$r_\beta = \frac{\partial \beta}{\partial t} + u_i \frac{\partial \beta}{\partial x_i} - u_3, \quad i = 1,2.$$

In the above, u_i is the velocity along the ith global reference axis, p is the dynamic pressure ($\bar{p} = \rho(p - gz)$ where $\bar{p}$ is the total pressure, ρ is the density and g is the gravity acceleration, β is the wave elevation, and τ_{ij} are the deviatoric viscous stresses related to the kinematic viscosity μ by the standard expression

$$\tau_{ij} = \mu \left(\frac{\partial u_i}{\partial x_j} + \frac{\partial u_j}{\partial x_i} - \delta_{ij} \frac{2}{3} \frac{\partial u_k}{\partial x_k} \right). \tag{4}$$

The boundary conditions for the stabilized problem are written as

$$n_j \tau_{ij} - t_i + \frac{1}{2} h_j n_j r_{m_i} = 0 \quad \text{on} \quad \Gamma_t \tag{5}$$

$$u_j - u_j^p = 0 \quad \text{on} \quad \Gamma_u \tag{6}$$

where n_j are the components of the unit normal vector to the boundary and t_i and u_j^p are prescribed tractions and displacements on the boundaries Γ_t and Γ_u, respectively.

The underlined terms in Eqs. (1)–(3) introduce the necessary stabilization for the numerical solution. Additional time stabilization terms can be accounted for in Eqs. (1)–(3), [4,5,9], although they have been found unnecessary for the type of problems solved here.

The *characteristic length* distances h_j represent the dimensions of the finite domain where balance of momentum and mass is enforced, [4,8]. The characteristic distances h_{β_j} in Eq. (3) represent the dimensions of a finite domain surrounding a point where the velocity is constrained to be tangent to the free surface, [2,9].

Equations (1)–(6) are the starting point for deriving a variety of stabilized numerical methods for solving the incompressible Navier-Stokes equations with a free surface using equal-order interpolations for the velocities, the pressure, and the wave height, [1–4,8,9].

Fractional Step Approach

Let us discretize in time the stabilized momentum Eq. (1*a*) as

$$\frac{u_i^{n+1} - u_i^n}{\Delta t} + \frac{\partial}{\partial x_j}(u_i u_j)^n + \frac{\partial p^n}{\partial x_i} - \frac{\partial \tau_{ij}^n}{\partial x_j} - \frac{1}{2} h_j \frac{\partial r_{m_i}^n}{\partial x_j} = 0. \tag{7}$$

A fractional-step method can be simply derived by splitting Eq. (7) as follows:

$$u_i^* = u_i^n - \Delta t \left[\frac{\partial}{\partial x_j}(u_i u_j) - \frac{\partial \tau_{ij}}{\partial x_j} - \frac{1}{2} h_j \frac{\partial r_{m_i}}{\partial x_j} \right]^n \tag{8}$$

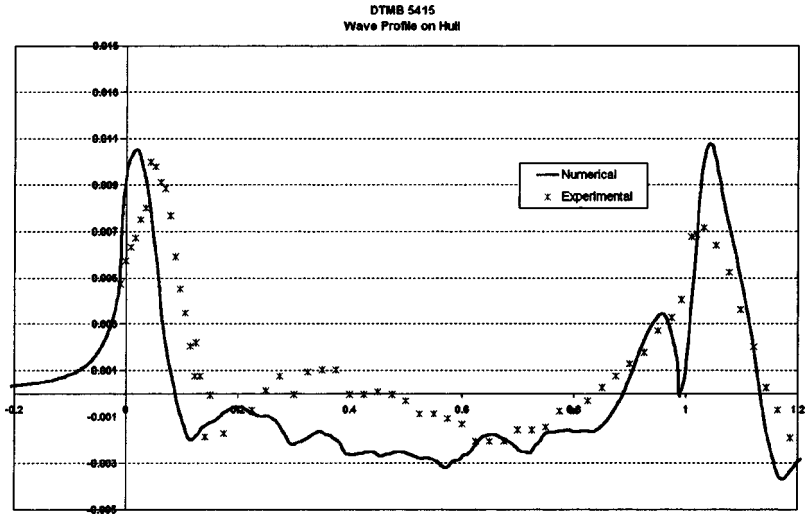

Fig. 4 DTMB 5415 model. Wave profile on the hull.

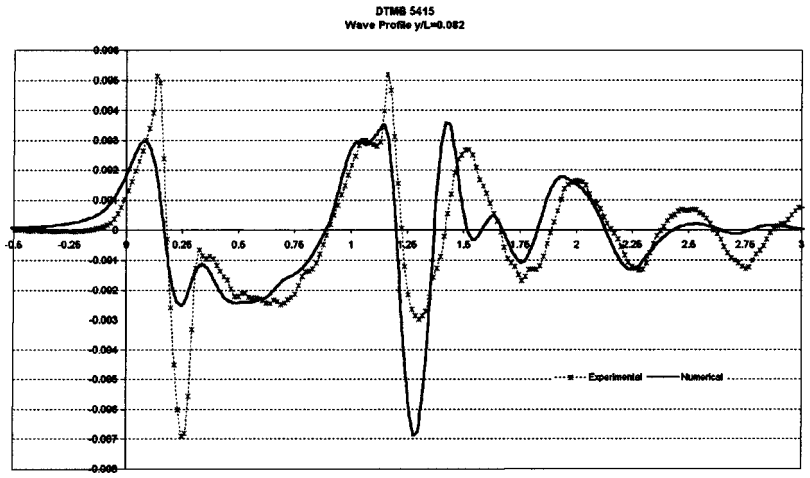

Fig. 5 DTMB 5415 model. Wave profile at $y/L=0.082$. -*- experimental values, [24]. –numerical results.

$$u_i^{n+1} = u_i^* - \Delta t \frac{\partial p^n}{\partial x_i}. \tag{9}$$

Note that addition of Eqs. (8) and (9) gives the original stabilized momentum Eq. (7).

Substitution of Eq. (9) into Eq. (2) gives

$$\Delta t \frac{\partial^2 p^n}{\partial x_i \partial x_i} = \frac{\partial u_i^*}{\partial x_i} - \tau_i u_i \frac{\partial r_d^n}{\partial x_i} \tag{10}$$

where τ_i are intrinsic time parameters defined as $\tau_i = h_i/2u_i$.

The free surface wave Eq. (3) can be also discretized in time to give, [2,7,9],

$$\beta^{n+1} = \beta^n - \Delta t \left[u_i^n \frac{\partial \beta^n}{\partial x_i} - u_3^n - \frac{1}{2} h_{\beta j} \frac{\partial r_\beta^n}{\partial x_j} \right] \quad i,j = 1,2. \tag{11}$$

Pressure Stabilization

Using Eq. (1) and neglecting high-order terms it can be obtained:

$$u_i \frac{\partial}{\partial x_i}\left(\frac{\partial u_j}{\partial x_j}\right) = \frac{\partial r_{m_i}}{\partial x_i}. \tag{12}$$

Substituting Eq. (12) into Eq. (10) gives

$$(\Delta t + \tau_i)\frac{\partial^2 p^n}{\partial x_i \partial x_i} = \frac{\partial u_i^*}{\partial x_i} - \tau_i \left[\frac{\partial r_i'}{\partial x_i}\right]^n \tag{13}$$

with

$$r_i' = \frac{\partial u_i}{\partial t} + \frac{\partial (u_i u_j)}{\partial x_j} - \frac{\partial \tau_{ij}}{\partial x_j} \quad i,j = 1,2,3. \tag{14}$$

Equation (13) is used to compute the pressure. The left-hand side is a Laplacian equation for the pressure values at time n, whereas the right-hand side includes known values of the fractional velocities, the velocities and the viscous stresses at time n.

Remark 1. Standard fractional step procedures neglect the contribution from the terms involving τ_i in Eq. (13). These terms improve the stabilization properties of the algorithm as they ensure the solution of Eq. (13) when the values of Δt are small. Also the influence of the τ_i terms has proven to be essential for obtaining improved and fully converged solutions in steady-state problems.

The finite calculus procedure can be also applied to derive a stabilized pressure increment split scheme. This can be simply derived by splitting Eq. (7) only for the pressure increment similarly as described in [2,7,9].

Remark 2. In Eq. (13) the cross derivative terms of the pressure have been neglected. These terms can be accounted for if a proper definition of the τ_i parameters is used. For details see [8].

Remark 3. The residual r_i' can be discretized using the finite elements method, [15] as

$$r_i' = \mathbf{N}\bar{\mathbf{r}}_i' \tag{15}$$

where $\mathbf{N} = [N_1, N_2, \cdots, N_n]$ contains the shape functions N_j and $(\bar{\cdot})$ denotes nodal values.

Application of the Galerkin method to Eq. (13) gives after integration by parts

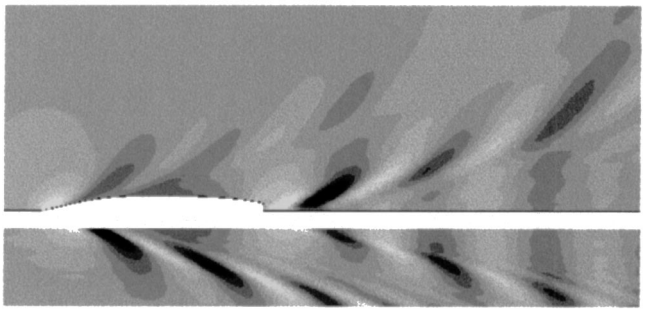

Fig. 6 Wave map of the DTMB 5415 model obtained in the simulation (above) compared to the experimental data (below)

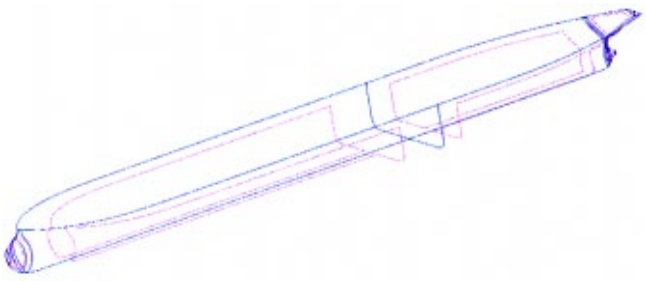

Fig. 7 KVLCC2 model. Geometrical definition based on NURBS surfaces.

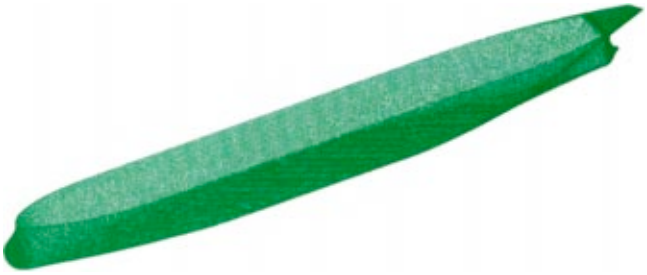

Fig. 8 KVLCC2 model. Surface mesh used in the analysis.

$$H_{kl}\bar{p}_l^n = \int_\Omega \frac{\partial N_k}{\partial x_i} u_i^* d\Omega - \int_\Omega \frac{\partial N_k}{\partial x_i} \mathbf{N}\bar{\mathbf{r}}_i'^n d\Omega \tag{16}$$

where $H_{kl}=\int_\Omega(\Delta t+\tau_i)\partial N_k/\partial x_i(\partial N_l/\partial x_i)d\Omega$ is the standard Laplacian matrix.

The values of r_i' can now be computed by projecting the pressure gradients. Neglecting the stabilization terms in Eq. (1) we can write

$$r_i' = -\frac{\partial p}{\partial x_i}. \tag{17}$$

Application of the Galerkin method to Eq. (17) gives using Eq. (15)

$$\mathbf{M}\bar{\mathbf{r}}_i'^n = \mathbf{q}^n \tag{18a}$$

with

$$M_{kl} = \int_\Omega N_k N_l d\Omega \quad \text{and} \quad q_k^n = -\int_\Omega N_k \frac{\partial p^n}{\partial x_i} d\Omega. \tag{18b}$$

Equation (18*a*) can be solved for the values of $\bar{\mathbf{r}}_i'^n$ using an iterative Jacobian scheme.

Remark 4. The above formulation can also be aplied to the Reynolds (RANSE) equations. In this case the value of r_{m_i} in the stabilized momentum equations is given by, [7]:

$$r_{m_i} = \frac{\partial u_i}{\partial t} + \frac{\partial}{\partial x_j}(u_i u_j) + \frac{\partial p}{\partial x_i} - \frac{\partial(\tau_{ij}^n + \tau_{R_{ij}}^n)}{\partial x_j} \tag{19}$$

where τ_R^n is the Reynolds stress tensor. In this work τ_R^n has been modeled using the standard Boussinesq's approximation.

Remark 5. The value of the intrinsic time parameters τ_i have been taken as, [8,9],

$$\tau_i = \left(\frac{4\mu}{3h_i^2} + \frac{2u_i}{h_i}\right)^{-1}. \tag{20}$$

Equation (20) provides the standard values of the intrinsic time parameter for the convective limit ($u_i \to 0$) and the viscous limit ($\mu \to 0$).

The characteristic length distances h_i are defined here using the SUPG assumptions giving, [4,8,16],

$$\mathbf{h} = \begin{Bmatrix} h_1 \\ h_2 \\ h_3 \end{Bmatrix} = h\frac{\mathbf{u}}{|\mathbf{u}|} \tag{21}$$

where $h=[V^{(e)}]^{1/3}$, where $V^{(e)}$ is the volume of the tetrahedral element.

The characteristic lenght distances $h_{\beta i}$ in the free-surface Eqs. (3) are defined by an identical expression to Eq. (21) with $h=[A^{(e)}]^{1/2}$, $A^{(e)}$ being the area of the triangular element over the sea surface.

More details on the computation of the stabilization parameters can be found in [4–10].

Finite Element Discretization

Space discretization is carried out using the finite element method, [15]. A linear interpolation over four-node tetrahedra for both u_i and p is chosen in the examples shown in next section. Similarly, linear triangles are chosen to interpolate β on the free-surface mesh.

The discretized integral form in space is obtained by applying the standard Galerkin procedure to Eqs. (8), (13), (9), and (11) and the boundary conditions (5) and (6). Solution of the discretized problem follows the pattern given below.

Step 1. Solve Eq. (8) for the nodal fractional velocities. The Dirichlet boundary conditions on the nodal velocities are imposed when solving Eq. (8). Note that the fractional step method can be interpreted as a Neumann boundary type Mixed formulation of the parabolic problem, [14,17].

Step 2. Solve Eq. (13) for the nodal pressures at time n+1. The pressures computed from Step 4 are used as a boundary condition

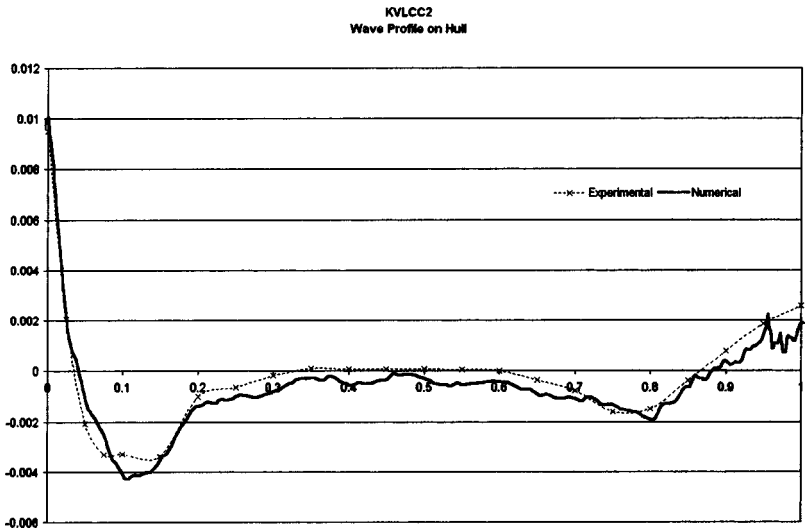

Fig. 9 KVLCC2 model. Wave profile on the hull compared to experimental data, [25]. Thick line shows numerical results.

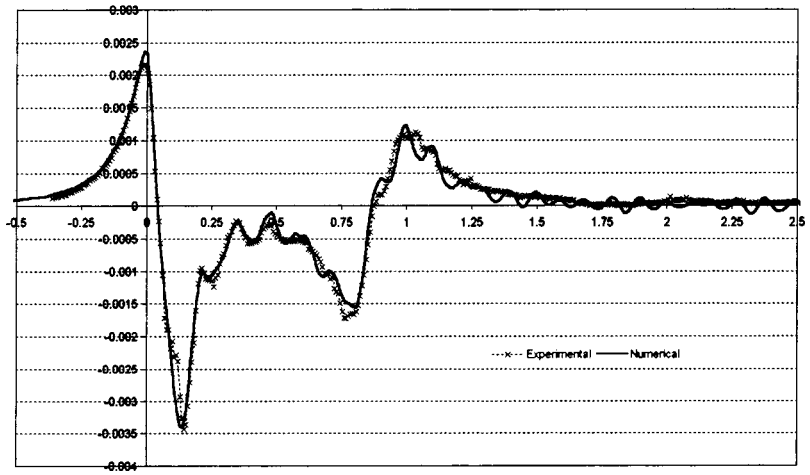

Fig. 10 KVLCC2 model. Wave profile on a cut at $y/L=0.0964$ compared to experimental data, [25]. Thick line shows numerical results.

Fig. 11 KVLCC2 model. Map of the X component of the velocity on a plane at 2.71 m from the orthogonal aft. Comparison with the experimental data, [25].

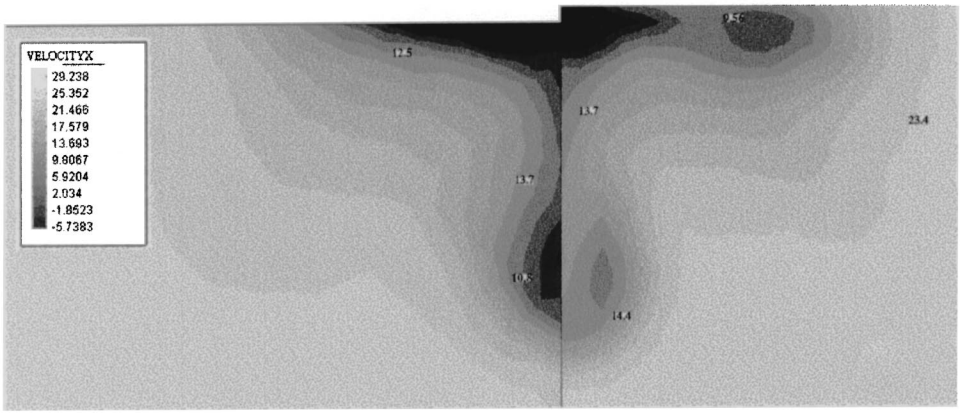

Fig. 12 KVLCC2 model. Map of the X component of the velocity on a plane at 2.82 m from the orthogonal aft. Comparison with the experimental data, [25].

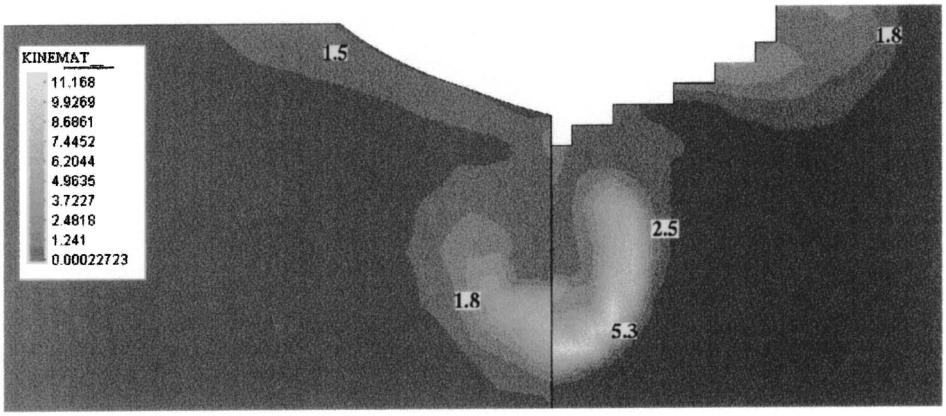

Fig. 13 KVLCC2 model. Map of the eddy kinetic energy (K) on a plane at 2.71 m from the orthogonal aft. Comparison with the experimental data, [25].

Fig. 14 *Bravo España* sail racing boat. Mesh used in the analysis.

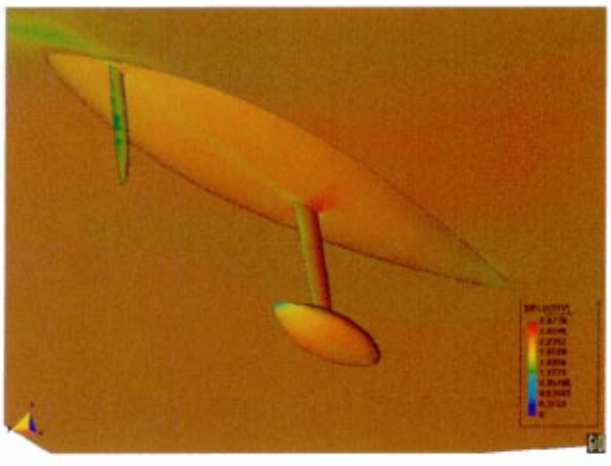

Fig. 15 *Bravo España*. Velocity contours.

for solution of Eq. (13) (viz. Eq. (18)).

Step 3. Solve Eq. (9) for the nodal velocities at time n+1. The Dirichlet boundary conditions on the nodal velocities are imposed when solving Eq. (9).

Step 4. Solve for the new free surface height at time n+1. The new free-surface elevation β^{n+1} in the fluid domain is computed from Eq. (11).

The pressure at the free surface is obtained from the balance of tractions at the surface, [18],

$$n_j \rho \tau_{ij} - n_i \bar{p} = n_j \rho_a \tau_{ij}^a - n_i \bar{p}^a + n_i \frac{\gamma}{R} \tag{22}$$

where $\bar{p}$ is the pressure field on water, $\bar{p}^a$ is the air pressure, τ_{ij}^a is the air viscous stress tensor, ρ_a is the air density, γ is the surface tension coefficient, R is the average curvature radius of the free surface, and n_i is the vector in the normal direction to the free surface. Assuming $\partial\beta/\partial x \ll 1$ and $\partial\beta/\partial y \ll 1$ it can be taken $\mathbf{n} = [0,0,-1]$.

In Eq. (22) the turbulent stresses are neglected close to the free surface as shown experimentally, [18,19].

Assuming that air is at rest ($p^a = 0$ and $\tau_{ij}^a = 0$), Eq. (22) can be simplified as

$$n_j \rho \tau_{ij} - n_i \bar{p} = n_i \frac{\gamma}{R}. \tag{23}$$

The third component of above equation gives

$$\bar{p} = \rho \tau_{33} + \frac{\gamma}{R}. \tag{24}$$

The dynamic pressure is finally obtained from

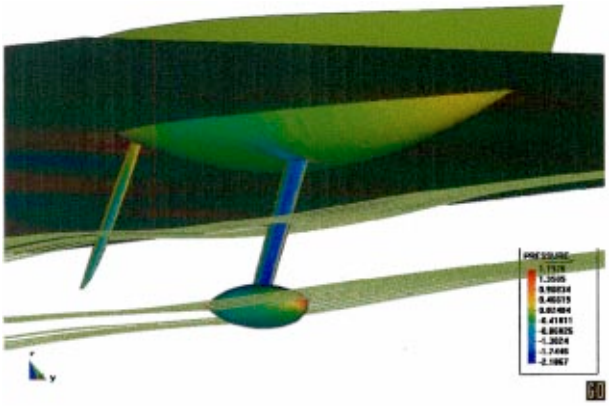

Fig. 16 *Bravo España*. Streamlines.

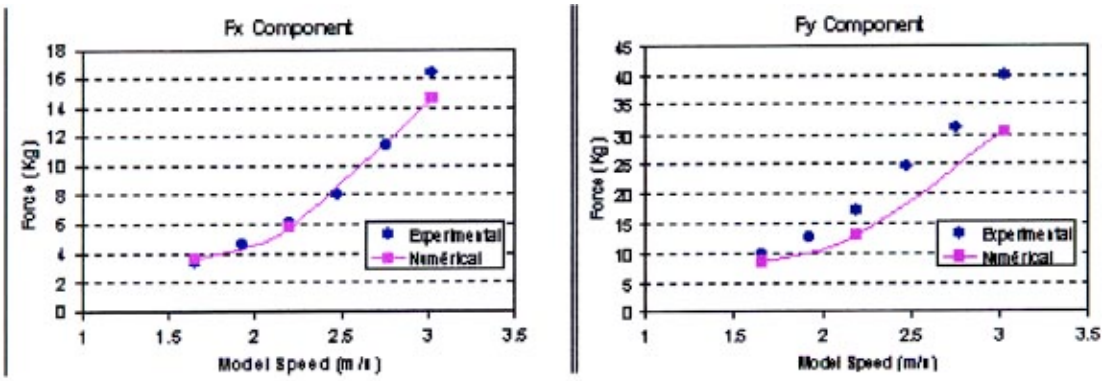

Fig. 17 ***Bravo España*. Resistance test. Comparison of numerical results with experimental data.**

$$p = \tau_{33} - \frac{\gamma}{\rho R} + g\beta \tag{25}$$

where g is the modulus of the acceleration of the gravity.

Reaching this point the fluid domain has to be updated due to the new position of the free surface. This is an expensive process and a simplified solution can be found by neglecting the change of the free surface and taking into account its effects by prescribing the pressure acting on the free surface. In order to increase the accuracy of the solution, the free-surface equation is modified by making use of a Taylor series expansion of β in the Oz direction, [20].

Remark 6. The conceptually simplest way to carry out the mesh updating due to the new position of the free surface and of the ship is by remeshing the new fluid domain. A number of algorithms for computation of moving boundaries and interfaces including free-surface flows using interface-tracking and interface-capturing techniques and remeshing algorithms have been proposed in recent years, [13,21]. Indeed, the use of tetrahedra elements and unstructured grids simplifies this process. However, remeshing is nowadays too expensive if industrial applications of the algorithms are sought.

Chiandussi, Bugeda, and Oñate [22] have proposed a simple method for movement of mesh nodes ensuring minimum element distorsion, thereby reducing the need of remeshing. The method is based on the iterative solution of a fictitious linear elastic problem on the mesh domain. In order to minimize mesh deformation the "elastic" properties of each mesh element are adequately selected so that elements suffering greater distortions are stiffer. Applications of this technique to ship hydrodynamic problems can be found in [3,7,9].

Transom Stern Model

It is well known that the transom flow occuring at a sufficient high speed has a singularity for the standard solution of the free-surface Eq. (11). Several authors have proposed solutions to these problem, [23,24], mainly based on experimental observations of this phenomena. Next, a more natural solution to solve the transom flow is presented.

The standard solution of convective equations such as the free-surface equation requires prescribing the Dirichlet conditions at the inflow. As the transom causes a discontinuity in the domain, the solution of the free-surface equation close to this region is inconsistent with the convective nature of the equation. The direct solution of the free surface equation in this case results in the instability of the wave height close to the transom region. This instability is found experimentally for low speeds. The flow at a sufficient high speed is physically more stable although it still cannot be reproduced by standard numerical techniques.

The solution to this problem is to apply adequate free-surface boundary conditions at the transom boundary. The obvious condition is to fix both the free-surface elevation β and its derivative along the corresponding streamline to values given by the transom position and the surface gradient. However, prescribing those values can influence the transition between the transom flux and the lateral flux, resulting in unaccurate wave maps.

The method here proposed is to extend the free surface below the ship. In this way the neccesary Dirichlet boundary conditions imposed at the inflow domain are enough to achieve the well-possessed properties of the problem. We note that is not an ad hoc condition, as Eq. (11) has to be satisfied also in the wetted surface below the ship. Obviously, this way to proceed is valid both for the wetted and dry transom cases and it can be also applied to ships with regular stern. In Fig. 1 the nodes marked with "*a*" include the standard degrees-of-freedom (β) of the free-surface problem; those nodes marked with "*b*" introduce the new degrees-of-freedom, while wave elevation β is prescribed at the nodes marked as "*c*."

Indeed, accounting for every surface element of the wetted ship surface is not neccesary. Just the first row of elements is enough as shown in all the numerical tests carried out without affecting the results.

This scheme can not be used in the case of partially wetted transom when the flow remains adhered to the transom instead of a detatched flow. These phenomena usually appear for highly unsteady flows where wake vortex induces the deformation of the free surface. To favor the convergence of the free surface to a stable state an artificial viscosity term has been added to the free-surface equations in the vecinity of the transom in these cases.

Examples

All examples have been solved in a standard single processor PC using the computer code SHYNE, [25] based on the algorithm here presented and the pre/postprocessor *GiD* developed at CIMNE, [26]. Recent industrial applications of the CFD formulation presented can be found in [27].

Example 1. DTMB 5415 Model. The first case analyzed is the David Taylor Model Basin 5415 benchmark model. The geometry used in the analysis was obtained from the Gothenburg 2000 Workshop database, [28]. The NURBS definition is shown in Fig. 2. The obtained results are compared with experimental data available, [28]. The main characteristics of the analysis are

- length: 5.72 m, beam: 0.5 m, draught: 0.248 m, wetted surface: 4.861 m^2,
- velocity: 2.1 m/seg, Froude number: 0.28, and
- viscosity: 0.001 Kg/mseg, density: 1000 Kg/m^3, Reynolds number: 12.310^6.

The analysis was carried out for three different grids (from 150,000 to 600,000 linear tetrahedra, corresponding to 25,000 and 115,000 nodes) in order to qualitatively analyze the influence of the element size in the solution. Here only the results corresponding to the finest grid are shown. The smallest element size used was 0.002 m and the maximum 0.750 m. The surface mesh of the DTMB 5415 used in the last analysis is shown in Fig. 3. The Smagorinsky turbulence model with the extended law of the wall was chosen. The tramsom stern flow model presented was used.

Figures 4 and 5 show the wave profile on the hull and in a cut at $y/L = 0.082$, respectively. Numerical results obtained are compared with the experimental data.

Figure 6 shows the comparison of the wave map obtained with the experimental data available.

Example 2. KVLCC2 Model. The next example is the analysis of the KVLCC2 benchmark model. Here a partially wetted tramsom stern is expected due to the low Froude number of the test. Figure 7 shows the NURBS geometry used obtained from the Hydrodynamic Performance Research team of Korea (KRISO). The obtained results are compared with the experimental data available in the KRISO database, [29].

The smallest element size used was 0.001 m and the largest 0.50 m. The surface mesh chosen is shown in Fig. 8. A total of 550,000 tetrahedra were used in the analysis. The tramsom stern flow model presented in the previous section was used.

Test 1. Wave pattern calculation. The main characteristics of the analysis are listed below:

- length: 5.52 m, beam (at water plane): 0.82 m, draught: 0.18 m, wetted surface: 8.08 m^2,
- velocity: 1.05 m/seg, Froude number: 0.142, and
- viscosity: 0.00126 Kg/mseg, density: 1000 Kg/m^3, Reynolds number: 4.6310^6.

The turbulence model used in this case was the K model. Figures 9 and 10 show the wave profiles on the hull and in a cut at $y/L = 0.082$ obtained in Test 1, compared to the experimental data. The obtained results are quantitatively good close to the hull. A lost of accuracy is observed in the profiles away from the hull. This is probably due to the fact that the element sizes are not small enough in this area.

Test 2. Wake analysis at different planes. Several turbulence models were used (Smagorinsky, K, and K-ϵ model) in order to verify the quality of the results. Here, only the results from the K-ϵ model are shown. We note that the velocity maps obtained even for the simplest Smagorinsky model were qualitatively good, showing the accuracy of the fluid solver scheme used. The main characteristics of this analysis are listed below:

- length: 2.76 m, beam (at water plane): 0.41 m, draught: 0.09 m, wetted surface: 2.02 m^2,
- velocity: 25 m/seg, Froude number: 0.0, and
- viscosity: 3.0510^{-5} Kg/mseg, density: 1.01 Kg/m^3, Reynolds number: 4.6310^6.

Figures 11 to 13 present the results corresponding to the Test 2. Figures 11 and 12 show the contours of the axial (X) component of the velocity on planes at 2.71 m and 2.82 m from the orthogonal aft, respectively. Figure 13 shows the maps of the kinetic energy on the first of these planes. Experimental results are shown for comparison in all cases.

Example 3. AMERICAN CUP BRAVO ESPAÑA Model The final example is the analysis of the Spanish American Cup racing sail boat *Bravo España*. The finite element mesh used is shown in Fig. 14. The results presented in Figs. 15–17 correspond to the analysis of a nonsymmetrical case including appendages. Good comparison between the experimental data and the numerical results was again obtained.

Conclusions

The finite calculus method provides modified forms of the governing differential equations for a viscous fluid with a free surface. Solution of the modified equations with a semi-implicit fractional step finite element method provides a straight forward and stable algorithm for analysis of ship hydrodynamic problems.

Numerical results obtained in the three-dimensional viscous analysis of complex ship geometries indicate that the proposed numerical method can be used with confidence for practical hydrodynamic design purposes in naval architecture.

Acknowledgments

Financial support for this work was provided by the European Community through projects Brite-Euram BR 967-4342 SHEAKS and Esprit 24903 FLASH. Thanks are given to Dr. H. Sierra from many useful suggestions. The authors are also grateful to Copa America Desafio Español SA for providing the geometry and experimental data of the racing boat analyzed.

Thanks are also given to Mr. J.A. Arráez for his help in computing some of the examples presented.

The authors also thank Prof. S. Idelsohn, Prof. R. Lohner, and Dr. C. Sacco for many useful discussions.

References

[1] García, J., Oñate, E., Sierra, H., Sacco, C., and Idelsohn, S., 1998, "A Stabilized Numerical Method for Analysis of Ship Hydrodynamics," *ECCOMAS98*, K. Papaliou et al., eds., John Wiley and Sons, New York.

[2] Oñate, E., Idelsohn, S., Sacco, C., and García, J., 1998, "Stabilization of the Numerical Solution for the Free Surface Wave Equation in Fluid Dynamics," *ECCOMAS98*, K. Papaliou et al., eds., John Wiley and Sons, New York.

[3] Oñate, E., and García, J., 1999, "A Methodology for Analysis of Fluid-Structure Interaction Accounting for Free Surface Waves," European Conference on Computational Mechanics (ECCM99), Aug. 31–Sept. 3, Munich, Germany.

[4] Oñate, E., 1998, "Derivation of Stabilized Equations for Advective-Diffusive Transport and Fluid Flow Problems," Comput. Methods Appl. Mech. Eng., **151**, pp. 233–267.

[5] Oñate, E., García, J., and Idelsohn, S., 1997, "Computation of the Stabilization Parameter for the Finite Element Solution of Advective-Diffusive Problems," Int. J. Numer. Methods Fluids, **25**, pp. 1385–1407.

[6] Oñate, E., García, J., and Idelsohn, S., 1998, "An Alpha-Adaptive Approach for Stabilized Finite Element Solution of Advective-Diffusive Problems With Sharp Gradients," *New Adv. in Adaptive Comp. Met. in Mech.*, P. Ladeveze and J. T. Oden, eds., Elsevier, New York.

[7] García, J., 1999, "A Finite Element Method for Analysis of Naval Structures," Ph.D. thesis, Univ. Politècnica de Catalunya, Dec. (in Spanish).

[8] Oñate, E., 2000, "A Stabilized Finite Element Method for Incompressible Viscous Flows Using a Finite Increment Calculus Formulation," Comput. Methods Appl. Mech. Eng., **182**, pp. 1–2, 355–370.

[9] Oñate, E., and García, J., 2001, "A Finite Element Method for Fluid-Structure Interaction With Surface Waves Using a Finite Calculus Formulation," Comput. Methods Appl. Mech. Eng., **191**, pp. 635–660.

[10] Oñate, E., 2001, "Possibilities of Finite Calculus in Computational Mechanics," presented at the First Asian-Pacific Congress on Computational Mechanics, APCOM'01 Sydney, Australia, Nov. 20–23.

[11] Tezduyar, T. E., 1991, "Stabilized Finite Element Formulations for Incompressible Flow Computations," Adv. Appl. Mech., **28**, pp. 1–44.

[12] Zienkiewicz, O. C., and Codina, R., 1995, "A General Algorithm for Compressible and Incompressible Flow. Part I: The Split Characteristic Based Scheme," Int. J. Numer. Methods Fluids, **20**, pp. 869–885.

[13] Tezduyar, T. E., 2001, "Finite Element Methods for Flow Problems With Moving Boundaries and Interfaces," Arch. Comput. Methods Eng., **8**, pp. 83–130.

[14] Codina, R., 2001, "Pressure Stability in Fractional Step Finite Element Methods for Incompressible Flows," J. Comput. Phys., **170**, pp. 112–140.

[15] Zienkiewicz, O. C., and Taylor, R. C., 2000, *The Finite Element Method*, 5th Ed., Butterworth-Heinemann, Stonetam, MA.

[16] Hughes, T. J. R., and Mallet, M., 1986, "A New Finite Element Formulations for Computational Fluid Dynamics: III. The Generalized Streamline Operator for Multidimensional Advective-Diffusive Systems," Comput. Methods Appl. Mech. Eng., **58**, pp. 305–328.

[17] Perot, J. B., 1993, "An Analysis of the Fractional Step Method," J. Comput. Phys., **108**, pp. 51–58.

[18] Alessandrini, B., and Delhommeau, G., 1999, "A Fully Coupled Navier-Stokes Solver for Calculation of Turbulent Incompressible Free Surface Flow Past a Ship Hull," Int. J. Numer. Methods Fluids, **29**, pp. 125–142.

[19] Celik, I., Rodi, W., and Hossain, M. S., 1982, "Modelling of Free Surface Proximity Effects on Turbulence," *Proc. Refined Modelling of Flows*, Paris.

[20] Idelsohn, S., Oñate, E., and Sacco, C., 1999, "Finite Element Solution of Free

Surface Ship-Wave Problem,'' Int. J. Numer. Methods Eng., **45**, pp. 503–508.
[21] Löhner, R., Yang, C., Oñate, E., and Idelsohn, S., 1999, ''An Unstructured Grid-Based Parallel Free Surface Solver,'' Concr. Library Int., **31**, pp. 271–293.
[22] Chiandusi, G., Bugeda, G., and Oñate, E., 2000, ''A Simple Method for Update of Finite Element Meshes,'' Commun, Numer. Meth. Engng., **16**, pp. 1–9.
[23] Matusiak, J., Tingqiu, L., and Lehtimäki, R., 1999, ''Numerical Simulation of Viscous Flow With Free Surface Around Realistic Hull Forms With Free Surface Around Realistic Hull Forms With Transform,'' Report of Ship Laboratory, Helsinki University of Technology, Finland.
[24] Raven, H. C., 1996, ''A Solution Method for Ship Wave Resistance Problem,'' Ph.d. thesis, University of Delft, June.
[25] García, J., 2002, ''SHYNE Manual,'' available at www.cimne.upc.es/shyne.
[26] ''GiD,'' 2001, The Personal Pre/Postprocessor, user manual available at www.gid.cimne.upc.es.
[27] Tdyn, 2002, ''A Finite Element Code for Fluid-Dynamic Analysis,'' COMPASS Ingeniería y Sistemas SA, www.compassis.com.
[28] David Taylor Model Basis 5415 Model Database, http://www.iihr.uiowa.edu/gothenburg2000/5415/combatant.html.
[29] Korea Research Institute of Ships and Ocean Engineering (KRISO), http://www.iihr.uiowa.edu/gothenburg2000/KVLCC/tanker.html.